forests

MDPI

Article

Effects of Oak Processionary Moth (*Thaumetopoea processionea* L.) Outbreaks on the Leaf Performance and Health of Urban and Forest Oak Trees (*Quercus robur* L.) in Brandenburg, Germany

Anne L. M. Arnold, Conor McGrath and Annett Reinhardt *

Department of Soil Science of Temperate and Boreal Ecosystems, Faculty of Forest Sciences and Forest Ecology, University of Goettingen, 37077 Goettingen, Germany
* Correspondence: annett.reinhardt@uni-goettingen.de

Abstract: Forest insects are among the most important factors of disturbance in European forests. The increase in and duration of drought stress events due to climate change not only increase the vulnerability of rural and urban forests but also predispose weakened stands to insect pest calamities. In this context, many German and European forest research institutes and environmental institutions report an increase in the densities and calamity developments of the oak processionary moth (*Thaumetopoea processionea* L.) not only in oak and mixed-oak forests but also in smaller areas where oak trees regularly occur, e.g., parklands, urban areas, copses, avenues, recreational forests, etc. It is expected that the oak processionary moth (OPM) will benefit from the overall weakened vitality of both individual oaks and oak stands in the future and that mass outbreaks will occur at an increased frequency. This paper reports on the effects that the OPM can have on tree performance for rural forest and urban oak trees by applying the chlorophyll fluorescence non-destructive diagnostic method for the identification and quantification of damage to oak leaves. The aim of the study was to investigate the effects of OPM frass activity on tree leaf health using chlorophyll fluorescence measurements, comparing infested host oaks with non-infested oaks in urban and forest environs. The study assessed: 1. the quantum efficiency of photosystem II (PS II), which counts as an indicator for leaf conditions, 2. the performance index, which indicates the efficiency of the photosynthetic light reaction, 3. the energy loss of the photosynthetic reaction, which is an indicator for cell damage, and 4. the degree of open reaction centers in PS II, which indicates how well light energy can be absorbed for photosynthesis. Infested urban and rural oaks showed a significantly reduced quantum yield of PS II by up to 10% compared to non-infested oak leaves. The leaf performance was significantly reduced by up to 35% for infested urban oaks and by up to 60% for infested forest oaks, respectively. The energy losses were two times higher for infested urban and forest oaks. However, OPM infestation led to a higher reduction in the photosynthetic performance in the leaves of forest oaks compared to that of urban oaks. In order to avoid permanent damage, suitable countermeasures must be taken quickly, as, immediately after pest infestation, the performance decreases significantly. A lower performance means a significant loss in biomass production as well as in tree vitality.

Keywords: chlorophyll fluorescence; JIP test; oak processionary moth; infested; non-infested oaks; urban and forest host trees; leaf health

check for updates

Citation: Arnold, A.L.M.; McGrath, C.; Reinhardt, A. Effects of Oak Processionary Moth (*Thaumetopoea processionea* L.) Outbreaks on the Leaf Performance and Health of Urban and Forest Oak Trees (*Quercus robur* L.) in Brandenburg, Germany. *Forests* **2023**, *14*, 124. https://doi.org/10.3390/f14010124

Academic Editors: Mateja Germ and Ivan Kreft

Received: 16 December 2022
Revised: 2 January 2023
Accepted: 3 January 2023
Published: 10 January 2023

Copyright: © 2023 by the authors. Licensee MDPI, Basel, Switzerland. This article is an open access article distributed under the terms and conditions of the Creative Commons Attribution (CC BY) license (https://creativecommons.org/licenses/by/4.0/).

1. Introduction

There is strong evidence that several insect pest species have altered their geographical range over the last few decades [1,2] due to the impact of climate change but also to human activity with respect to the commercial movement of infested (nursery) trees as well as the ongoing loss and fragmentation of insect pest species habitats [3].

In conjunction with this, one of the most current and major defoliator insect pests, presently established in almost every European country, is the oak processionary moth

(OPM) (*Thaumetopoea processionea* L.). OPM population dynamics seem unpredictable [4], and outbreak events can lead to the massive destruction of forests. During outbreaks, the larvae of the caterpillars are also particularly harmful to people and livestock as a result of the large quantity of urticating setae that they release into the environment [5]. Larvae produce setae containing toxic thaumetopoein from the third instar onward. These setae easily break when larvae move and remain toxic for several years in the environment as well as in exuviae and old nests. When touched or inhaled, they cause the release of histamines in humans, which can result in extreme allergic reactions [6]. The natural biocontrol of OPM is limited due to the toxicity of the larvae. Hence, they are avoided by vertebrate predators such as birds and mammals [6].

Historically, the habitat of the OPM has been limited to southern areas, but since the 1980s, it has been expanding northwards and to large areas in the Netherlands, the UK, Germany, Belgium and France; additionally, far northern and southern Sweden [7] are at risk. According to the German State Institutes of Forestry and Health Protection Centers, severe OPM infestations in the federal states have been a problem around urban environs since 2005, when OPM spread to forests in regions such as Bavaria and Brandenburg and caused heavy defoliation. The current and potential establishment of OPM poses a new and difficult management problem for arborists, local authorities, contractors and tree/forest owners [8]. In order to assess the resilience of infested oaks, this study was carried out to compare infested and non-infested oak leaves in urban and forest environs.

It is expected that the geographical expansion of OPM will continue to increase dramatically, which is attributed to climate warming [5]. The changing temperature and precipitation patterns not only significantly affect the reproduction cycle of different insect pest species but also cause changes in water availability for trees. The evapotranspiration (water consumption) of trees in urban and rural landscapes will increase with elevated air temperatures and solar radiation. The impact of drought on exchanges at the soil–root and canopy–atmosphere interfaces (e.g., from water and CO_2 flux measurements) resulted in a reduction in transpiration and water uptake. Furthermore, modifications in chlorophyll and leaf pigments and in net carbon assimilation (i.e., decreasing photosynthesis) [9] result in stomatal closure [10]. This combination of declining precipitation and reduced soil water reservoirs coupled with the increasing water consumption will induce severe limitations of water availability for plants (i.e., drought stress). This will severely affect the metabolism of plants by lowering photosynthetic activity, which will subsequently cause a reduction in biomass productivity, i.e., net ecosystem production (NEP) as well as net primary production (NPP), and therefore above-ground carbon sequestration [11,12].

The photosynthetic process involves the conversion of solar energy to chemical energy through a chain of biological systems. The efficiency of this process is determined by many environmental parameters such as light, temperature and nutrient and water availability. Infections with pathogens, fungi, bacteria or viruses create particular stress conditions that can damage parts of the photosynthetic apparatus and thus reduce the photosynthetic capacity and efficiency of the affected plant [13].

The plant photosynthetic process consists of two phases: the light and the dark reaction. In the light reaction, light energy is transferred to chlorophylls and is used via an electron transport chain, through protein complexes in the thylakoid membranes of the chloroplasts, to transfer electrons from water via various intermediate stations such as plastoquinone to oxidized nicotinamide adenosine dinucleotide phosphate (NADP) [13].

In the light-dependent reaction at PS II, in the thylakoid membrane of chloroplasts, light energy is transformed to split water and activate chlorophyll electrons that travel through the electron transport chain to the cytochrome-complex and photosystem I (PS I). From PS I, electrons are transferred non-cyclically to ferredoxin or cyclically, if PS II is non-functional (e.g., to protect the system from photodamage due to excessive light), to cytochrome to transform the electric energy in chemical energy, creating reduced nicotinamide adenosine dinucleotide phosphate NADPH [13].

In the case of chlorophyll, in addition to the desired output (the transfer of electrons to the electron transport chain), energy is also released in the form of heat and/or fluorescence. A technique that has been used for decades to determine the photosynthetic performance of plants is the detection of this chlorophyll fluorescence [13].

One can make practical use of the property of chlorophyll fluorescence to measure photosynthetic activity non-destructively via a biophysical method. Chlorophyll fluorescence detection can be used to make determinations about the state of PS II and the course of the light reaction and can be used to investigate the stress physiology of plants [14]. Plant stress response examination via chlorophyll fluorescence to abiotic stress, i.e., light [15], drought [16–19], heat [20,21], chilling [20,22,23] freezing [23,24] and biotic stress, i.e., leaf chewing insects [25,26], gall formers and fungi [27,28], is well reported. Nevertheless, most investigations have been conducted under lab conditions with perennial plants or tree saplings to avoid the complex environmental conditions inherent to natural systems [27].

In situ measures of chlorophyll fluorescence on leaves of adult trees in forests affected by pests, especially the OPM-pest on oaks, are rare. Dormant for many decades, the sudden spread of OPM and increase in Europe and Germany is currently a major issue facing oaks. Heavy defoliation leads to weakened oak trees and forests but also, because of the setae on larvae, to severe itching and allergic reactions among people and livestock [29]. Generally, insect frass activity damages leaves and leads to disrupted stoma, damaged cell walls, disorganized protoplasts and granular cytoplasm and disintegrated chloroplasts, nuclei and phloem [20].

In contrast to the conventional measurement method of chlorophyll fluorescence via Pulse Amplitude Modulation (PAM), the detection of direct fluorescence with the most modern measuring instruments (Plant Efficiency Analyzer (PEA)) according to the OJIP method, where the different stages of the polyphasic fluorescence transient are marked alphabetically with O, J, I and P, enables a precise analysis and evaluation of the physiological state and efficiency of photosynthesis. In the so-called "open" (O) state (=F0), the fluorescence quantum yield of the system is minimal in the darkened leaf, as an incoming photon of actinic light from the PEA has a maximal chance to initiate a charge separation in one of the reaction centers. After illumination, electrons will travel through the electron chain: plastoquinone A (Q_A), plastoquinone B (Q_B) and the pool of free plastoquinone (PQ) from PS II to PS I. The fluorescence quantum yield will be increased because further incoming photons cannot be accepted by the partially saturated electron transport chain. When the majority of electrons in the reaction centers (RC) of a leaf have reduced the Q_A molecules in these reaction centers, the "J" state of the fluorescence kinetics has been reached. When Q_B is also reduced, the "I" level of the fluorescence quantum yield is reached. Once the PQ pool has reached its peak of reduction, the fluorescence quantum yield also reaches its peak at the so called "P" step [30] (see also Table 1). The short duration of a single measurement enables a high repetition rate (up to 200 measurements per hour) [31]. The method is also used in environmental protection. Here, for example, the degree of damage to trees can be measured [32,33].

Table 1. Definitions of terms and formulas for the calculation of parameters from chlorophyll *a* fluorescence transient OJIP.

O, J, I, P	**Nomenclature of the JIP-Test; Fluorescence Values at Different Points in Time of the Fast Fluorescence Kinetics, from the Origin to the Peak with Intermediate Steps; Characteristic Points Used for Calculations to Describe the Shape of the Kinetics.**
F_t	Fluorescence at time t after the onset of actinic illumination
$F_{50\mu s} = F_O = F_0$	Minimal fluorescence at 50 µs, the Origin of the onset of actinic illumination (F zero)
$F_{2ms} = F_J$	Fluorescence intensity at 2 ms, at the intermediate step "J"; this marks the point of the first stabile electron acceptor within the electron transport cascade (QA) at the end of Photosystem II.
$F_{30ms} = F_I$	Fluorescence intensity at 30 ms, at the intermediate step "I", the PSI electron acceptor side. This marks the beginning of the electron transport cascade of Photosystem I.

Table 1. *Cont.*

O, J, I, P	Nomenclature of the JIP-Test; Fluorescence Values at Different Points in Time of the Fast Fluorescence Kinetics, from the Origin to the Peak with Intermediate Steps; Characteristic Points Used for Calculations to Describe the Shape of the Kinetics.
$F_P = F_M$	Maximal recorded fluorescence intensity at the peak "P" of the fast fluorescence kinetics.
$\varphi_{Po} = TR_0/ABS = F_V/F_M$	Maximum quantum yield for primary photochemistry
$\Psi_{Eo} = ET_0/TR_0 = (1 - V_J)$	Probability that a photon trapped by the PSII reaction center enters the electron transport chain further than Q_A^-.
$\varphi_{Eo} = ET_0/ABS = [1 - (F_0/F_M)]\ \Psi_{Eo}$	Quantum yield of electron transport from PS II to the electron-acceptor side of PS I.
$M_0 = 4\ (F_{300\mu s} - F_{50\mu s})/(F_M - F_0)$	Initial slope (per millisecond) of the fluorescence kinetics normalized on the maximal variable fluorescence F_V.
$RC/ABS = \varphi_{Po}\ (V_J/M_0)$	Q_A reducing (active) RCs per PSII antenna Chl; measure for the activity of reaction centers.
10RC/ABS	The value of RC/ABS multiplied by 10 to shift the values in a range; more reachable.
$TR_0/RC = M_0\ (1/V_J)$	Trapped energy flux (leading to Q_A reduction) per reaction center.
$DI_0/RC = ABS/RC - TR_0/RC = [M_0(1/V_J)(1/\varphi_{Po})] - [M_0(1/V_J)]$	Dissipated energy flux per RC; measure for energy loss.
$PI_{ABS} = (RC/ABS)[\varphi_{Po}/(1 - \varphi_{Po})][\Psi_{Eo}/(1 - \Psi_{Eo})]$	Performance index (potential) for energy conservation from photons absorbed by PSII to the reduction in intersystem electron acceptors.

This paper reports on the effects caused by insect mass outbreaks of the most current and major defoliator and insect pest on oak—the oak processionary moth (*Thaumetopoea processionea* L.)—and on what impact this pest can have on the photosynthetic system in OPM-infested and non-infested leaves by comparing the photosynthetic activity/efficiency of oak leaves on infested trees and those on non-infested trees in urban and forest environs.

2. Material and Methods

2.1. Test Sites

The effects of OPM on the photosynthetic performance and stress response of common oak (*Quercus robur*) leaves were studied at one forest area (forest) and in one urban area (urban) in the cultural landscape of Westhavelland, which is located within the meadowlands of the Havellaendisches Luch in the Federal state of Brandenburg, Germany. The forest test site is approximately 900 m^2 and is located near Stölln on the Gollenberg (52°44′34″ N, 12°23′51″ E). Trees (approximately 73 years old, with an average height of 21 m, growing on clayey glacial sand) were chosen randomly. The urban test site located in Rathenow (52°36′15″ N, 12°21′39″ E) was adjacent to a highly frequented street, a supermarket parking lot, and a school. Due to the high level of anthropogenic influence, the soil on the urban site was classified as a non-further-classified-anthrosol. Urban oaks were 70–75 years old and had an average height of 23 m. Trees from within this group were also randomly selected. At both the forest and urban sites, non-infested oak leaves were compared to oak leaves currently infested with OPM during the 2016 and 2017 vegetation periods.

The infestation level was determined with an egg survey on twigs in crowns [34] and a caterpillar slip control with a degree of egg-parasitism from information provided by Dr. K. Möller (Center for Forest Research (LFE), Department Forest Protection Brandenburg). Trees were also observed visually with binoculars and monitored throughout the frass activity period to determine the level of infestation. This was estimated to be 60% of the leaf loss in 2016 and 85% in 2017.

Measurements were conducted in two consecutive years, 2016 and 2017, at comparable leaves (sun crown, measurement height, leaf area) on the same tress, based on a repeated measurement design. Leaf parameters were examined monthly from May to October during the vegetation period from leaf-shoot to senescence. For the respective sites (forest and urban), 12 trees were selected and divided into infestation categories (infested and non-infested), providing 6 trees per infestation level per site. From each tree, 30 leaves were sampled to determine their photosynthetic performance and stress response. Leaf-level measurements were performed between 10:00 a.m. and 2:00 p.m.

2.2. Measurements and Sampling

All measured leaves were dark-adapted for 30 min using Hansatech leaf clips prior to the Chl *a* fluorescence measurement with a Plant Efficiency Analyzer (Pocket PEA chlorophyll fluorimeter, Hansatech Instruments Ltd., King's Lynn, UK). The emitter wavelength of a non-modulated light source was 625 nm for the actinic light LED. High-quality optical band pass filters were used for the detector (Chl *a* fluorescence 730 ± 15 nm). Measurements were performed on circular areas of the leaves measuring 2 mm in diameter, using leaf clips homogeneously illuminated by actinic light LEDs set to a saturating light intensity of 3.500 µmol photons m^2/s. The detection of Chl *a* fluorescence was recorded within five different time intervals: every 10 µs for the initial fluorescence (0–300 µs), every 100 µs (0.3–3 ms), 1 ms (3–30 ms), 10 ms (0.03–0.3 s) and 100 ms (0.3–1 s). Raw data were transferred and processed using PEA Plus 1.0 software (Hansatech Instruments Ltd.). For the interpretation of differences in the Chl *a* fluorescence induction curves, the fluorescence values were normalized to F_0 = 50 µs. The primary photochemistry of PS II was further evaluated using the well-established parameters described in Table 1. The changes in these parameters are associated with various stressors as well as the overall plant vitality. In order to have full control over all calculations, all parameters were calculated in spreadsheets and optimized for a high-throughput workflow of Chl *a* fluorescence raw data using Libre Office 6 (The Document Foundation, Berlin, Germany). The data were plotted graphically using Prism 8 for Mac OS-X software (GraphPad Software Inc., La Jolla, CA, USA) (for the definitions of terms, see Table 1).

2.3. JIP Test

The different stages of the polyphasic fluorescence transient are marked alphabetically with O, J, I and P. The analysis of the transient is called the JIP test and was used to compare the averaged chlorophyll fluorescence kinetics (Chl II—fluorescence) of infested leaves (red curves) with those of non-infested leaves (green curves) (Figure 1). In most months of the study, the measurement curves were similar in their course. The level of the fluorescence signal at the end of the one-second recording of the fluorescence kinetics gives conclusions about the functionality of the photosynthetic electron transport chain (light reaction). A lower signal indicates disturbances in the electron transport capacity, which can be traced back to the effect of stressors.

2.4. The Photosynthetic Performance

The photosynthetic performance is described by the quantum yield of PS II (PHI Po), the Performance Index PI_{ABS}, the energy loss and the degree of opening of the reaction centers. This parameter represents the physiological status of PS II in the photosynthetic system according to [35]. The performance index P I_{ABS} is calculated as the product of independent parameters combining the density of PS II RCs, the quantum efficiency of primary photochemistry and the conversion of excitation energy into electron transport [35].

2.5. Reaction Centers' Activity

Once light is absorbed by the PS II antenna complexes, energy is transferred to the PS II RCs, and, if in an open state (oxidized state), they are "active" to convert light energy to chemical energy [36]. The activity of RCs can be determined by the factor RC/ABS [37]. For better scaling, this factor is multiplied tenfold.

2.6. Statistical Data Analysis

Raw data were transferred and processed using PEA Plus software (Hansatech Instruments Ltd.). The maximum quantum yield of PS II (PHI Po) was calculated for F_0 = 50 µs. Chl-a fluorescence induction curves were analyzed to determine the performance index (PI total), the Q_A reducing reaction centers (RC) per PS II antenna chlorophyll (RC/ABS) and the ratio of the total dissipation of untrapped excitation energy from all RCs with respect to the number of active RCs (DIo/RC) due to [38]. All calculations were performed

using the opensource software Libre Office 6 (The Document Foundation, Berlin, Germany). Prism 8 for Mac OS-X software (GraphPad Software Inc., La Jolla, CA, USA) was used for statistical analysis.

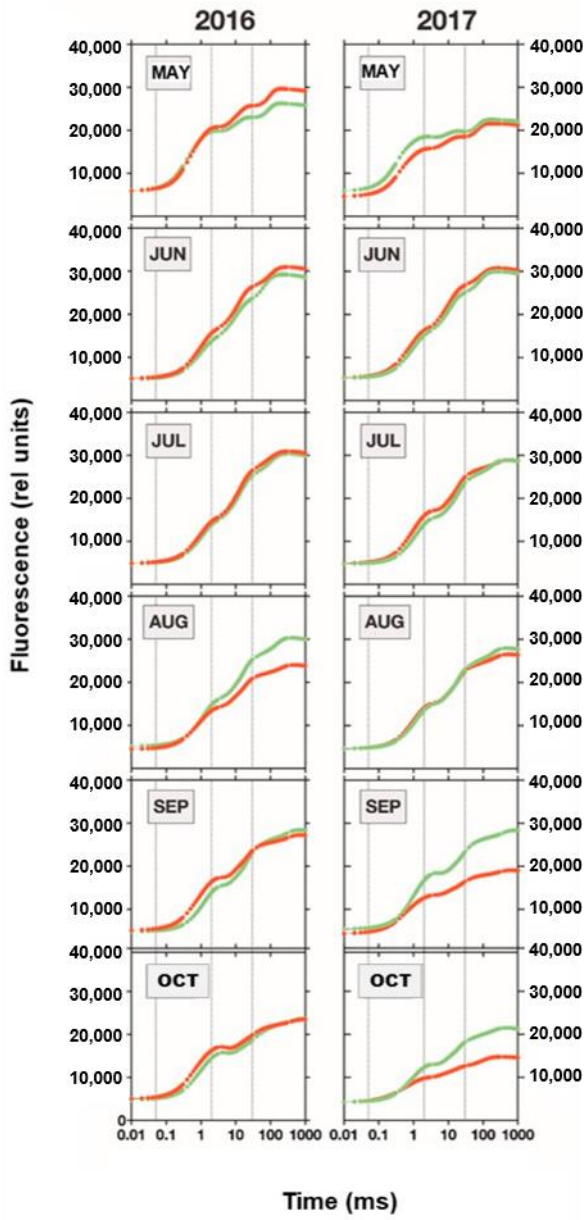


Figure 1. Fluorescence kinetics of PS II chlorophyll fluorescence; comparison of OPM-infested oak leaves (red curves) with non-infested ones (green curves) in the urban area of Rathenow, Brandenburg. May to October 2016 and 2017.

Prior to comparisons between treatments, all data were tested for the normal distribution and homogeneity of variances. Statistical analyses were performed using R package version 1.3.1 [39]. Differences between non-infested and infested sites were detected using the non-parametric Kruskal–Wallis test on ranks. For multiple pairwise comparison within one treatment at different sampling dates between the parameters and the infested vs. control sites at each sampling date, a post-hoc Dunn's test was performed using the Bonferroni correction for the *p*-value adjustment [40]. For statistical analyses, SPSS (SPSS Statistics for Windows, version 22.0., IBM, Armonk, NY, USA) was used. Comparisons between infested and non-infested sites, as well as sampling dates, were tested using ANOVA.

3. Results

3.1. Urban Trees in Rathenow

JIP Test

The results of the JIP test for the urban site are shown in Figure 1. There are significantly weaker signals of OPM-infested urban oak leaves in the months of August of 2016 and September and October of 2017, which are striking. Infested urban leaves showed a reduced number of active reaction centers in August 2016, with the same trend being observed in September and October 2017 compared to non-infested urban leaves. In contrast, the activation level of the reaction centers of non-infested urban leaves corresponds to the expected regular annual course. Under non-infested conditions, the fluorescence kinetics of PS II appeared to be the highest in August (2016) with 30,000 relative fluorescence units (RFU) and in 2017 with 29,000 RFU (June), while the lowest values appeared in October for both 2016 and 2017. Under infestation, the highest values were measured in June 2016, with 30,500 RFU, and the lowest were measured in October (2017), with 15,000 RFU. In contrast to the results from the forest site, the kinetical differences were less pronounced in urban leaves and appeared the highest in August (2016), with +20% for non-infested leaves, as well as September (2017), with +34%, and October (2017), with +29% in non-infested leaves. The fluorescence kinetics were temporarily higher under infestation (e.g., May and June 2016).

3.2. Quantum Yield of Photosystem II (PHI Po)

The quantum yield/quantum efficiency is normally above 80% (0.80) in fully developed, unstressed leaves. In May, when the leaves are still juvenile, the photosystems are not yet fully developed, which is reflected in a lower quantum yield (Figure 2a,b). From June to September, the leaves are fully developed, and in October, leaf aging begins, which is reflected in a decreasing quantum yield. The quantum efficiency of the leaves of infested trees is significantly worse than that of non-infested trees. For example, the quantum yield of infested leaves in October 2017 is 10% lower compared to that of non-infested trees. The ability to absorb light energy is lower and fluctuates. Senescence also begins earlier in infested leaves.

3.3. Performance Index PI_{ABS}

The greatest performance of the photosynthetic electron transport chain is typically expected in deciduous species in July, when the leaves are fully mature and the photosystems are fully functional. In July 2016, no significantly different values could be detected between the leaves of infested and non-infested trees (Figure 2c,d). In July of the following year (2017), however, highly significant differences were detected. The performance index PI_{ABS} of leaves of non-infested trees averaged 105, while infested trees had an average value of only 60, a 35% lower performance. This trend continued throughout the entire 2017 growing season. The leaf performance index for both 2016 and 2017 was highest for urban trees in June, with a decrease afterwards. Infested urban leaves showed a reduced performance during all sampling dates except for May in both years, where infested urban trees showed an enhanced leaf development compared to non-infested urban trees (Figure 2).

3.4. Energy Loss DIo/RC

When plants are under stress, energy is released by targeting heat to the photosynthetic reaction centers (RC) to prevent over-energization and damage to the protein complexes of the photosynthetic chain. After leaf emergence in May, leaves are not yet fully developed, so more energy must be dissipated (Figure 2e,f). Especially in August and September 2016, leaves of OPM-affected trees release 50% more energy than unaffected ones. In July 2017, the month in which the performance of infested leaves is reduced by 35% (see above), the RCs release significantly more energy (27%).

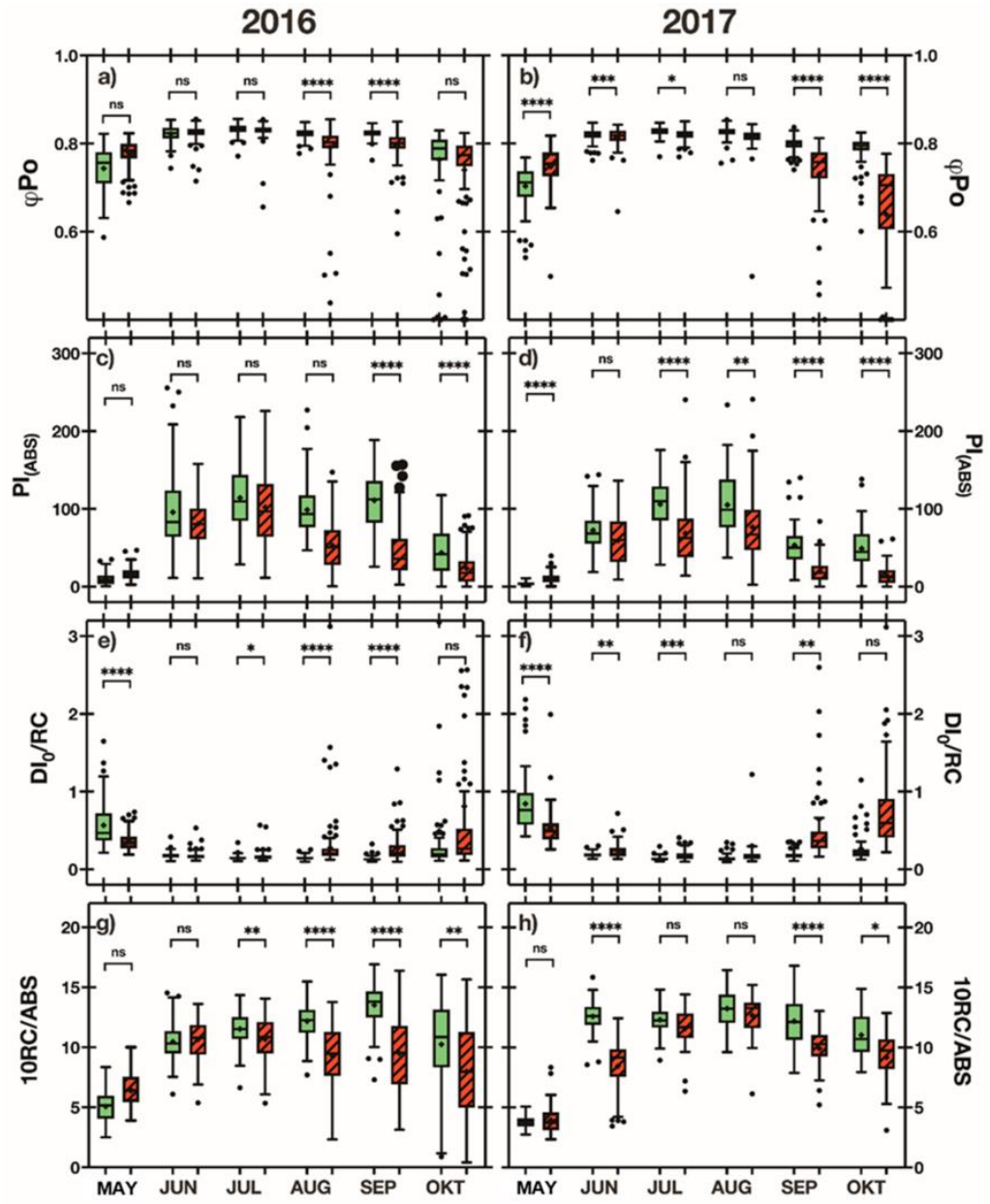


Figure 2. Comparison of photosynthetic performance and stress parameters. OPM-infested leaves of oaks (red colour) and of non-infested leaves (green colour) in the urban area of Rathenow, Brandenburg. May to October 2016 and 2017. (**a**,**b**) Po = PHI Po = Fv/Fm = quantum efficiency of PS II, indicator of general leaf condition. (**c**,**d**) PIABS = Performance Index, indicator for the efficiency of the photosynthetic light reaction up to the start of PS I. (**e**,**f**) DIo/RC = Energy loss of the photosynthetic reaction center, targeted heat release as protection against over-energetisation of the photosystem, protection against cell damage. (**g**,**h**) 10RC/ABS = Degree of opening of the reaction centres in PS II, which indicates how well light energy can be absorbed for photosynthesis. Displayed in boxplots with Tukey interval. Cross-lines in boxes, median. Crosses, mean values. Significances calculated by analysis of variance (one-way ANOVA). Significance level: ns = $p > 0.05$; * = $p < 0.05$; ** = $p < 0.01$; *** = $p < 0.001$; **** = $p < 0.0001$.

3.5. Degree of Opening of the Reaction Centers 10RC/ABS

In large parts of the 2016 growing season and in some months of the 2017 season, leaves of infested trees show a significantly reduced light receptivity compared to those of non-infested trees (Figure 2g,h). For example, in August 2016, 25% fewer reaction centers are open. Conversely, this means that 25% fewer reaction centers convert light energy

into chemical energy. The photosynthesis capacity is thus reduced, so less biomass can be formed.

3.6. Forest Trees at Gollenberg

JIP Test

Figure 3 shows the results of the JIP test for the forest site. For forest tree leaves infested with OPM, the reaction centers ability to convert light-energy is constantly lower compared to non-infested leaves. For non-infested leaves, the highest values were in 2016 in July, with 29,500 RFU, and in 2017, with 30,500 RFU. May of both years showed the lowest values, with 25,000 RFU (2016) and 22,000 RFU (2017). In infested leaves, the highest values were in 2016, with 27,000 RFU (June), and in 2017, with 26,000 RFU in July. The lowest results were measured in 2016, with 16,000 RFU (August), and in 2017, with 14,000 RFU in May. The fluorescence kinetics were more varied, with higher values under no infestation (when compared to infested leaves), with +46% in August and +47% in September (2016). In 2017, the values were +44% (June), +39% (August), +34% (September) and +47% (October).

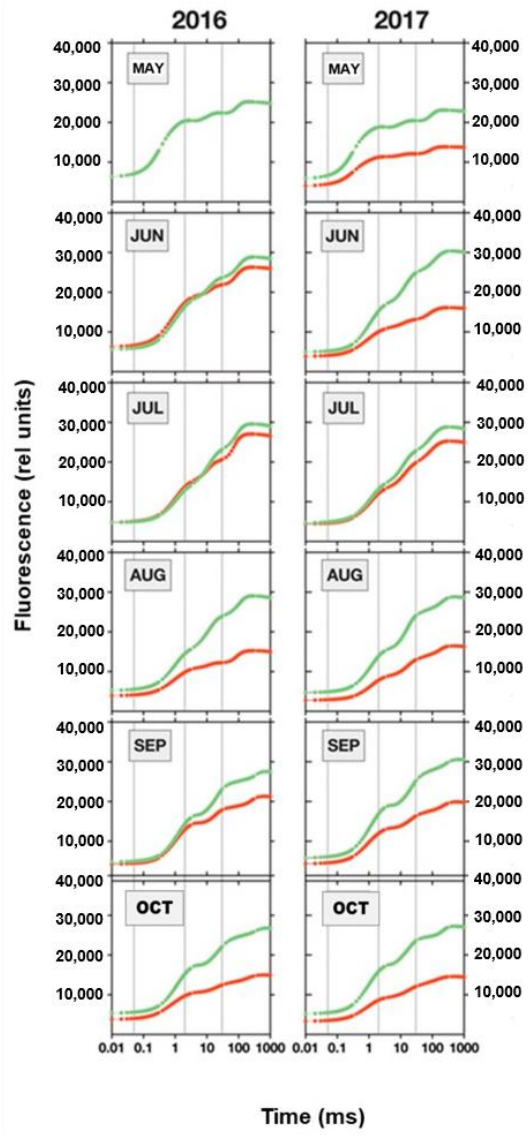


Figure 3. Fluorescence kinetics of PS II chlorophyll fluorescence, comparison of OPM-infested leaves of oaks (red curves) with leaves of non-infested ones (green curves) at Gollenberg, Rhinow, Brandenburg. May to October 2016 and 2017.

3.7. Quantum Yield of Photosystem II (PHI Po)

Immediately after the OPM infestation in June 2016, the quantum yield of the leaves of infested trees differed significantly from that of the leaves of non-infested trees (Figure 4a,b). The quantum yield of infested leaves in August 2016 was more than 10% lower than that of non-infested leaves. The ability to absorb light energy is significantly reduced throughout the growing season.

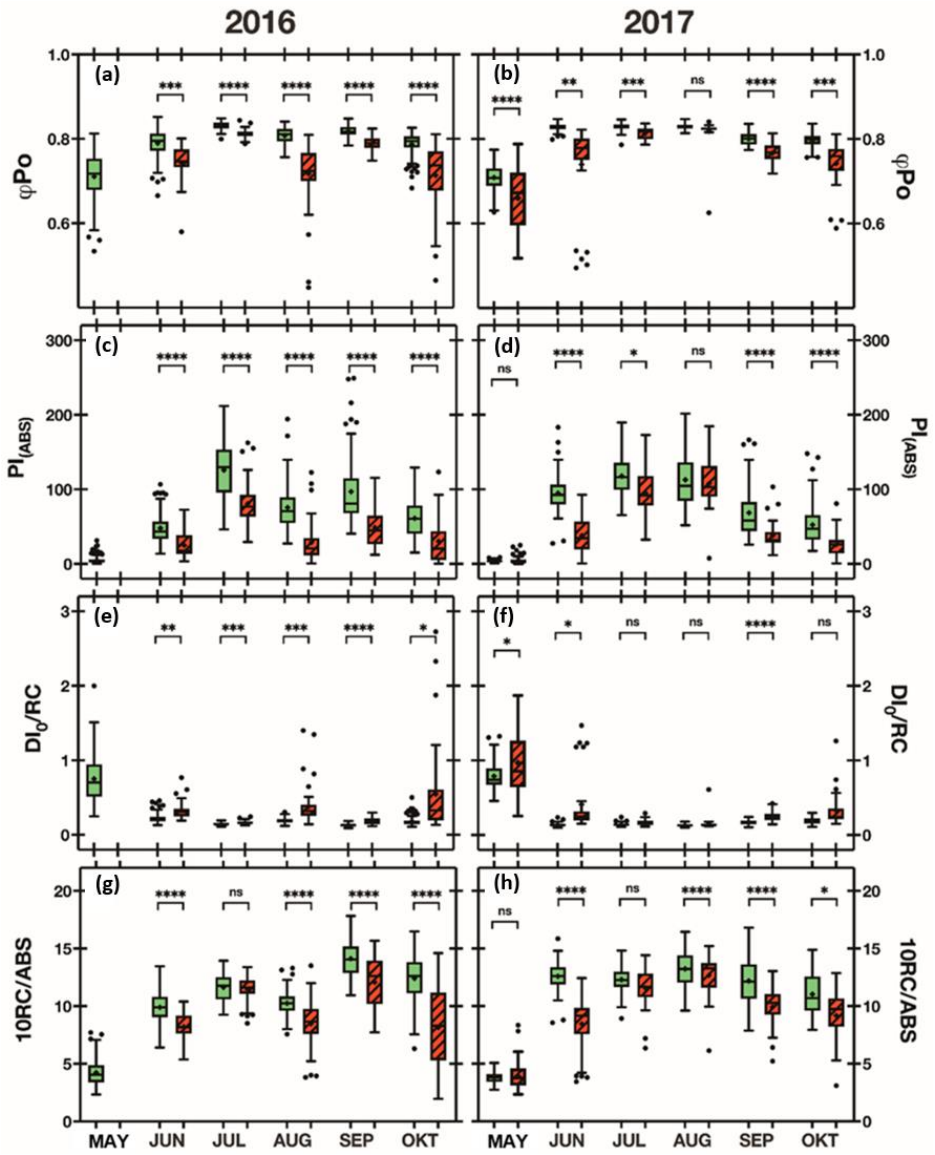


Figure 4. Comparison of photosynthetic performance and stress parameters. OPM-infested leaves of oak (red colour) and non-infested leaves (green colour) in a forest area. Stölln, Gollenberg, Brandenburg. May to October 2016 and 2017. (**a**,**b**) Po = PHI Po = Fv/Fm = quantum efficiency of PS II, indicator for the general condition of the leaves. (**c**,**d**) PIABS = Performance Index, indicator for the efficiency of the photosynthetic light reaction up to the start of PS I. (**e**,**f**) DIo/RC = Energy loss of the photosynthetic reaction centre, targeted heat release as protection against over-energisation of the photosystem, protection against cell damage. (**g**,**h**) 10RC/ABS = Degree of opening of the reaction centre in PS II, which indicates how well light energy can be absorbed for photosynthesis. Displayed in boxplots with Tukey interval. Cross-lines in boxes, median. Crosses, mean values. Significances calculated by analysis of variance (one-way ANOVA). Significance level: ns = $p > 0.05$; * = $p < 0.05$; ** = $p < 0.01$; *** = $p < 0.001$; **** = $p < 0.0001$.

3.8. Performance Index PI_{ABS}

Directly after OPM infestation, the performance is significantly reduced. In the main performance month of July (2016), it is reduced by 35% (Figure 4c,d). In August 2016, it was found to be more than 60% lower than that in non-infested leaves. This trend continues in the following year, especially at the beginning of the growing season and after the end of summer. In August 2017, however, the performance does not differ significantly. For leaves of *Q. robur* on the forest site, the performance index peaks in July and decreases afterwards. OPM-infested leaves on forest trees show a decreased performance index during all sampling dates in 2016, whereas in 2017, this was the case for June, July, September and October, while no difference was detectable during May and August (Figure 4).

3.9. Energy Loss DIo/RC

During the entire 2016 growing season, leaves of OPM-infested trees release significantly more energy than non-infested ones (Figure 4e,f). In August 2016, the month in which the performance of infested leaves is reduced by 60% (see above), the reaction centers release twice as much energy as they do in leaves of non-infested trees.

3.10. Degree of Opening of the Reaction Centers 10RC/ABS

In large parts of the 2016 growing season and in some months of the 2017 season, the leaves of infested trees show a significantly reduced light receptivity compared to those of non-infested trees. For example, in August 2016, 17% fewer reaction centers are open (Figure 4g,h).

4. Discussion

The aim of the study was to measure, non-destructively, the effects of leaf damage by OPM frass activity in terms of photosynthetic performance based on the biophysical measurement method of chlorophyll fluorescence by comparing infested host oaks with non-infested ones within urban and forest environs. The parameters assessed were: 1. the quantum efficiency of PS II, which is an indicator for leaf conditions, 2. the Performance Index, which indicates the efficiency of the photosynthetic light reaction, 3. the energy loss of the photosynthetic reaction centers, which is an indicator for cell damage, and 4. the degree of opening of the reaction centers in PS II, which indicates how well light energy can be absorbed for photosynthesis. The results show that the site conditions seem to be of great importance to how an oak stand can cope with OPM calamities. Particularly on sites with a poor water supply, such as the south-exposed dry slope on the Gollenberg, an OPM infestation is clearly noticeable in a reduction in performance across all indices. A lower performance means a decreased biomass production and a reduction in vitality. In the urban area of Rathenow, OPM infestation is not as noticeable in the physiology of infested leaves as it is at the Gollenberg forest site. However, the enormous loss of leaf mass due to feeding cannot be compensated for by the small number of remaining leaves.

At both locations, the photosynthetic performance and stress parameters show significant differences with respect to non-infested and infested leaves. Performance indices have proven to be highly sensitive to different abiotic stressors [22,35,41–46] as well as to biotic stress caused by insect infestations [47]. Based on the decreased performance of leaves infested by the OPM in 2016 and 2017, we can expect a decreased growth rate of these trees during the infestation.

OPM defoliation leads to a decreasing efficiency of the photosynthetic apparatus, with a reduced functioning of the electrons moving along the chains. The results indicate altered processes within the reaction centers such as light absorption (ABS), energy trapping (TR), electron transport (ET) and a decrease in the end electron acceptor (RE) [35]. The differences between infested and non-infested oaks were more pronounced at the forest test plot compared to the results gathered from infested and non-infested oaks in the urban area. Generally, the non-infested oaks showed relatively similar values across all measurements between the two

sites (when differing site conditions are taken into consideration). From this point of view, it is suggested that urban oaks are better adapted to the environmental conditions and more capable of tolerating the stresses induced by OPM infestation [19,20,48–51].

It is known that the environment and, thus, the climatic conditions influence the reaction norm of trees regarding their physiological processes. Studies have shown that trees in old forests or trees that have adapted to permanent climatic situations for a longer time have a larger fine root system than trees in younger forests or trees that were suddenly confronted with new environmental conditions [52]. Land-use-induced changes alter the size and morphology of the fine root system as a mechanism for regulating drought resistance in beech. It is thus clear that the "ecological memory" of trees and forests must be considered when assessing or predicting the sensitivity of forest ecosystems or urban trees to global environmental changes and the associated disturbances. Legacy effects therefore influence the response of tree growth to climate extremes [52,53]. On the other hand, a better performance of urban oaks might also be achieved based on an improved nutrient supply by anthropogenic fertilized depositions [45,54], genetical aspects [55] as well as the interaction between chlorophyll content and insect damage [56].

Different stresses can cause the transformation of PS II RCs to "heat sinks", where the excitation energy is dissipated as heat instead of being transformed to photochemical energy, where the parameter DI0/RC is a measure quantifying the dissipation of energy as heat via PS II RCs [38,57]. Non-infested leaves of urban trees emitted increased thermal radiation compared to the OPM-infested urban leaves only in May 2016 and 2017, when the leaves are not fully developed. In September, the heat emissions of infested leaves are increased compared to those of the non-infested leaves of urban and forest oak trees. The frass activity and leaf damage of the infested trees of both environments therefore led to a reduced photochemical energy.

The maximum quantum efficiency of PS II (Po; FV/FM), calculated as the ratio between the variable fluorescence (FM–F0) and the maximum fluorescence FM, is well known to describe the physiological state of photosynthesis [58]. Despite the introduction of models of a higher complexity [59], this formula is still widely used to quantify responses in plants to abiotic stress [15,16,60,61], as well as for biotic stress [62].

In 2016, the efficiency of PS II in leaves of infested trees in urban surroundings is significantly lower compared to that in non-infested leaves from July to October. In May and June of 2016 and May of 2017, the leaves of the infested urban trees were superior in their developmental state to those of the unaffected trees and therefore have a higher efficiency of PS II. In forests, the PS II efficiency of infested leaves was significantly lower compared to that of non-infested leaves during all sampling dates in both measured years. In May 2016, when the leaves are still juvenile, the photosystems are not yet fully developed, which reflects in low PHI Po values. From June to September, the leaves are fully developed, with maximum values for both infested and non-infested trees. In October, leaf senescence starts, but the leaf condition of infested trees is worse compared to that of non-infested ones. This means that the ability to absorb light energy is decreased and fluctuates more when trees are infested by OPM. Additionally, leaf senescence starts earlier, when trees are infested.

Leaf heat emissions are high in May 2016 due to the leaves not yet being fully developed, thus resulting in heat emission to protect the cells against radiation. In immature and undeveloped leaves (and their photosystems), excess light energy must be dispensed to ensure the integrity of the biomembranes in the thylakoids. The infestation with OPM means stress for the tree, which must be compensated for by the increased heat emissions compared to the non-infested trees. Therefore, the controlled heat emission is increased to protect the infested leaves from further damage. More energy must therefore be emitted unused, which otherwise would have promoted photosynthesis in healthy, unaffected leaves. The increased thermal radiation of infested leaves in September could be an indicator of the earlier leaf senescence caused by the OPM leaf destruction.

5. Conclusions

The results of this investigations show that forest oaks exhibit a greater degree of reduction in photosynthetic performance than urban oaks. It is assumed that urban oaks are already better adapted to stress conditions and have developed corresponding physiological adaptation mechanisms. In contrast to oaks in the forest, urban oaks experience permanent stress through higher temperatures and water deficits within the urban environment. This is caused by a lack of cooling by transpiration, increased heat convection and long-wave radiation from no vegetative surfaces by buildings and roads as well as chemical stresses form a variety of sources [63,64]. Therefore, stronger legacy effects at the urban tree scale, which influences the response of the tree reaction to climate extremes, and associated insect calamities are suggested. In this study, the chlorophyll fluorescence method was proved to be an effective and fast diagnostic method that can be applied quickly and in a stress-free manner to both forest and urban trees.

Author Contributions: Conceptualization, formal analysis, writing—original draft, visualization, supervision, project leading, funding acquisition, A.L.M.A., investigation, A.R., data curation, writing—review and editing, A.L.M.A. and A.R., writing—review and editing, A.L.M.A., A.R. and C.M. All authors have read and agreed to the published version of the manuscript.

Funding: This research was funded by the Federal Ministry of Education and Research (BMBF), project MOPM, funding number: 01LN1318A.

Data Availability Statement: The data presented in this study are available on request from the corresponding author.

Acknowledgments: We are grateful to the Federal Ministry of Education and Research (BMBF) for the project funding of the project MOPM (01LN1318A). We are also grateful to Christopher Brandt from the Climate Concept Foundation (CCF) in Hamburg and to Aline Wenning and Katrin Möller from the Forest Service Center Eberswalde (LFE), Department of Forest Protection. We acknowledge the support of the Open Access Publication Funds of the Göttingen University.

Conflicts of Interest: The authors declare no conflict of interest.

References

1. Robinet, C.; Roques, A. Direct impacts of recent climate warming on insect populations. *Integr. Zool.* **2010**, *5*, 132–142. [CrossRef] [PubMed]
2. Parmesan, C.; Ryrholm, N.; Stefanescu, C.; Hill, J.K.; Thomas, C.D.; Descimon, H.; Huntley, B.; Kaila, L.; Kullberg, J.; Tammaru, T.; et al. Poleward shifts in geographical ranges of butterfly species associated with regional warming. *Nature* **1999**, *399*, 579–583. [CrossRef]
3. Townsend, M.C. *Report on Survey and Control of Oak Processionary Moth Thaumetopoea processionea (Linnaeus) (Lepidoptera: Thaumetopoeidae)*; OPM: London/Oxford, UK, 2009.
4. Stigter, H.; Van Tol, W.J.H.M.; Spijkers, H.C.P. *Thaumetopea processionea* in the Netherlands: Present status and management perspectives (*Lepidoptera: Notodontidae*). In *Proceedings of the Section Experimental and Applied Entomology of the Netherlands Entomological Society*; Nederlandse Entomologische Vereniging: Amsterdam, The Netherlands, 1997; Volume 8, pp. 3–16.
5. Townsend, M. An outbreak of the Oak Processionary moth *Thaumetopoea processionea* (L.) (Lep.: *Thaumetopoeidae*) in south-west London. *Entomol. Rec. J. Var.* **2007**, *118*, 193.
6. Gottschling, S.; Meyer, S. An Epidemic Airborne Disease Caused by the Oak Processionary Caterpillar. *Pediatr. Dermatol.* **2006**, *23*, 64–66. [CrossRef] [PubMed]
7. EFSA. Evaluation of a pest risk analysis on *Thaumetopoea processionea* L., the oak processionary moth, prepared by the UK and extension of its scope to the EU territory. *EFSA J.* **2009**, *7*, EFSA-Q-2008-711. [CrossRef]
8. Bräsicke, N. Ökologische Schäden, gesundheitliche Gefahren und Maßnahmen zur Eindämmung des Eichenprozessionsspinners im Forst und im urbanen Grün. *Jul. -Kühn-Arch. Nr* **2012**, *6*, bis 07. [CrossRef]
9. Baldocchi, D.D.; Black, T.A.; Curtis, P.S.; Falge, E.; Fuentes, J.D.; Granier, A.; Gu, L.; Knohl, A.; Pilegaard, K.; Schmid, H.P.; et al. Predicting the onset of net carbon uptake by deciduous forests with soil temperature and climate data: A synthesis of FLUXNET data. *Int. J. Biometeorol.* **2005**, *49*, 377–387. [CrossRef]
10. Bréda, N.; Huc, R.; Granier, A.; Dreyer, E. Temperate forest trees and stands under severe drought: A review of ecophysiological responses, adaptation processes and long-term consequences. *Ann. For. Sci.* **2006**, *63*, 625–644. [CrossRef]
11. Ciais, P.; Reichstein, M.; Viovy, N.; Granier, A.; Ogée, J.; Allard, V.; Aubinet, M.; Buchmann, N.; Bernhofer, C.; Carrara, A.; et al. Europe-wide reduction in primary productivity caused by the heat and drought in 2003. *Nature* **2005**, *437*, 529–533. [CrossRef]

12. Desprez-Loustau, M.-L.; Marçais, B.; Nageleisen, L.-M.; Piou, D.; Vannini, A. Interactive effects of drought and pathogens in forest trees. *Ann. For. Sci.* **2006**, *63*, 595–610. [CrossRef]
13. Sonnewald, U. Stoffwechselphysiologie. *Strasburger—Lehrb. Der Pflanz.* **2014**, *V279656*, 337–446. [CrossRef]
14. Vlaovic, J.; Balen, J.; Grgic, K.; Zagar, D.; Galic, V.; Simic, D. An Overview of Chlorophyll Fluorescence Measurement Process, Meters and Methods. In Proceedings of the 2020 International Conference on Smart Systems and Technologies (SST), Osijek, Croatia, 14–16 October 2020; pp. 245–250. [CrossRef]
15. Sano, S.; Takemoto, T.; Ogihara, A.; Suzuki, K.; Masumura, T.; Satoh, S.; Takano, K.; Mimura, Y.; Morita, S. Stress Responses of Shade-Treated Tea Leaves to High Light Exposure after Removal of Shading. *Plants* **2020**, *9*, 302. [CrossRef] [PubMed]
16. del Pozo, A.; Méndez-Espinoza, A.M.; Romero-Bravo, S.; Garriga, M.; Estrada, F.; Alcaíno, M.; Camargo-Rodriguez, A.V.; Corke, F.M.K.; Doonan, J.H.; Lobos, G.A. Genotypic variations in leaf and whole-plant water use efficiencies are closely related in bread wheat genotypes under well-watered and water-limited conditions during grain filling. *Sci. Rep.* **2020**, *10*, 460. [CrossRef] [PubMed]
17. Percival, D.; Murray, A.; Stevens, D. Drought stress dynamics of wild blueberry (*Vaccinium angustifolium* aiton). *Acta Hortic.* **2003**, *618*, 353–362. [CrossRef]
18. Koller, S.; Holland, V.; Brüggemann, W. Effects of drought stress on the evergreen *Quercus ilex* L., the deciduous *Q. robur* L. and their hybrid *Q.* × *turneri* Willd. *Photosynthetica* **2013**, *51*, 574–582. [CrossRef]
19. Percival, G. Evaluation of physiological tests as predictors of young tree establishment and growth. *J. Arboric. Urban For.* **2003**, *30*, 80–91. [CrossRef]
20. Percival, G. The use of chlorophyll fluoresecence to indentify chemical and environmental stress in leaf tissue of three oaks (*Quercus*) species. *J. Aboriculture* **2005**, *31*, 215–227. [CrossRef]
21. Yamada, M.; Hidaka, T.; Fukamachi, H. Heat tolerance in leaves of tropical fruit crops as measured by chlorophyll fluorescence. *Sci. Horti.* **1996**, *67*, 39–48. [CrossRef]
22. Gururani, M.A.; Venkatesh, J.; Tran, L.S.P. Regulation of Photosynthesis during Abiotic Stress-Induced Photoinhibition. *Mol. Plant* **2015**, *8*, 1304–1320. [CrossRef] [PubMed]
23. Ehlert, B.; Hincha, D.K. Chlorophyll fluorescence imaging accurately quantifies freezing damage and cold acclimation responses in *Arabidopsis* leaves. *Plant Methods* **2008**, *4*, 12. [CrossRef] [PubMed]
24. Zulini, L.; Fischer, C.; Bertamini, M. Chlorophyll fluorescence as a tool for evaluation of viability in freeze-stressed grapevine buds. *Photosynthetica* **2010**, *48*, 317–319. [CrossRef]
25. Aldea, M.; Hamilton, J.G.; Resti, J.P.; Zangerl, A.R.; Berenbaum, M.R.; Frank, T.D.; DeLucia, E.H. Comparison of photosynthetic damage from arthropod herbivory and pathogen infection in understory hardwood saplings. *Oecologia* **2006**, *149*, 221–232. [CrossRef] [PubMed]
26. Nabity, P.D.; Heng-Moss, T.M.; Higley, L.G. Effects of Insect Herbivory on Physiological and Biochemical (Oxidative Enzyme) Responses of the Halophyte *Atriplex subspicata* (*Chenopodiaceae*). *Environ. Èntomol.* **2006**, *35*, 1677–1689. [CrossRef]
27. Pérez-Bueno, M.L.; Pineda, M.; Barón, M. Phenotyping Plant Responses to Biotic Stress by Chlorophyll Fluorescence Imaging. *Front. Plant Sci.* **2019**, *10*, 1135. [CrossRef] [PubMed]
28. El Omari, B.; Fleck, I.; Aranda, X.; Moret, A.; Nadal, M. Effect of fungal infection on leaf gas-exchange and chlorophyll fluorescence in *Quercus ilex*. *Ann. For. Sci.* **2001**, *58*, 165–174. [CrossRef]
29. Groenen, F.; Meurisse, N. Historical distribution of the oak processionary moth *Thaumetopoea processionea* in Europe suggests recolonization instead of expansion. *Agric. For. Èntomol.* **2012**, *14*, 147–155. [CrossRef]
30. Küpper, H.; Benedikty, Z.; Morina, F.; Andresen, E.; Mishra, A.; Trtílek, M. Analysis of OJIP Chlorophyll Fluorescence Kinetics and Q_A Reoxidation Kinetics by Direct Fast Imaging. *Plant Physiol.* **2019**, *179*, 369–381. [CrossRef]
31. Murchie, E.H.; Lawson, T. Chlorophyll fluorescence analysis: A guide to good practice and understanding some new applications. *J. Exp. Bot.* **2013**, *64*, 3983–3998. [CrossRef]
32. Kalaji, H.M.; Jajoo, A.; Oukarroum, A.; Brestic, M.; Zivcak, M.; Samborska, I.A.; Cetner, M.D.; Łukasik, I.; Goltsev, V.; Ladle, R.J. Chlorophyll a fluorescence as a tool to monitor physiological status of plants under abiotic stress conditions. *Acta Physiol. Plant.* **2016**, *38*, 102. [CrossRef]
33. Rossini, M.; Panigada, C.; Meroni, M.; Colombo, R. Assessment of oak forest condition based on leaf biochemical variables and chlorophyll fluorescence. *Tree Physiol.* **2006**, *26*, 1487–1496. [CrossRef]
34. Delb, H.; Schröter, H.; Seemann, D. *Eichenprozessionsspinner—Waldschutz-Info 01/2002*; Forstliche Versuchs- und Forschungsanstalt Baden-Württemberg: Freiburg-Breisgau, Germany, 2005.
35. Strasser, R.J.; Srivastava, A.; Tsimilli-Michael, M. The Fluorescence Transient as a Tool to Characterize and Screen Photosynthetic Samples. In *Probing Photosynthesis: Mechanism, Regulation & Adaptation*; CRC Press: Boca Raton, FL, USA, 2000; pp. 443–480.
36. Kalaji, H.M.; Schansker, G.; Brestic, M.; Bussotti, F.; Calatayud, A.; Ferroni, L.; Goltsev, V.; Guidi, L.; Jajoo, A.; Li, P.; et al. Frequently asked questions about chlorophyll fluorescence, the sequel. *Photosynth. Res.* **2017**, *132*, 13–66. [CrossRef] [PubMed]
37. Strasser, R.J.; Tsimilli-Michael, M.; Srivastava, A. Analysis of the chlorophyll a fluorescence transient. In *Chlorophyll a Fluorescence: A Signature of Photosynthesis*; Papageorgiou, G.C., Govindjee, Eds.; Springer: Dordrecht, The Netherlands, 2004; pp. 321–362. [CrossRef]

38. Strasser, R.J.; Tsimilli-Michael, M.; Qiang, S.; Goltsev, V. Simultaneous in vivo recording of prompt and delayed fluorescence and 820-nm reflection changes during drying and after rehydration of the resurrection plant *Haberlea rhodopensis*. *Biochim. Biophys. Acta (BBA)—Bioenerg.* **2010**, *1797*, 1313–1326. [CrossRef]
39. *R Core Team: A Language and Environment for Statistical Computing*; European Environment Agency: Vienna, Austria, 2008.
40. Dinno, A. Nonparametric Pairwise Multiple Comparisons in Independent Groups using Dunn's Test. *Stata J. Promot. Commun. Stat. Stata* **2015**, *15*, 292–300. [CrossRef]
41. van Heerden, P.D.R.; Strasser, R.J.; Kruger, G.H.J. Reduction of dark chilling stress in N2-fixing soybean by nitrate as indicated by chlorophyll a fluorescence kinetics. *Physiol. Plant.* **2004**, *121*, 239–249. [CrossRef]
42. Schansker, G.; Tóth, S.Z.; Strasser, R.J. Dark recovery of the Chl a fluorescence transient (OJIP) after light adaptation: The qT-component of non-photochemical quenching is related to an activated photosystem I acceptor side. *Biochim. Biophys. Acta (BBA)—Bioenerg.* **2006**, *1757*, 787–797. [CrossRef] [PubMed]
43. Zivcak, M.; Olsovska, K.; Slamka, P.; Galambošová, J.; Rataj, V.; Shao, H.B.; Brestic, M. Application of chlorophyll fluorescence performance indices to assess the wheat photosynthetic functions influenced by nitrogen deficiency. *Plant Soil Environ.* **2014**, *60*, 210–215. [CrossRef]
44. Long, A.; Zhang, J.; Yang, L.-T.; Ye, X.; Lai, N.-W.; Tan, L.-L.; Lin, D.; Chen, L.-S. Effects of Low pH on Photosynthesis, Related Physiological Parameters, and Nutrient Profiles of *Citrus*. *Front. Plant Sci.* **2017**, *8*, 185. [CrossRef]
45. Zhang, W.W.; Niu, J.F.; Wang, X.K.; Tian, Y.; Yao, F.F.; Feng, Z.Z. Effects of ozone exposure on growth and photosynthesis of the seedlings of *Liriodendron chinense* (Hemsl.) Sarg, a native tree species of subtropical China. *Photosynthetica* **2011**, *49*, 29–36. [CrossRef]
46. Samborska, I.A.; Kalaji, H.M.; Sieczko, L.; Borucki, W.; Mazur, R.; Kouzmanova, M.; Goltsev, V. Can just one-second measurement of chlorophyll a fluorescence be used to predict sulphur deficiency in radish (*Raphanus sativus* L. sativus) plants? *Curr. Plant Biol.* **2019**, *19*, 100096. [CrossRef]
47. Gomes, A.M.S.D.V.; Reis, F.D.O.; De Lemos, R.N.S.; Mondego, J.M.; Braun, H.; Araujo, J.R.G. Physiological characteristics of citrus plants infested with citrus blackfly. *Rev. Bras. Èntomol.* **2019**, *63*, 119–123. [CrossRef]
48. Boshier, D.; Broadhurst, L.; Cornelius, J.; Gallo, L.; Koskela, J.; Loo, J.; Petrokofsky, G.; Clair, B.S. Is local best? Examining the evidence for local adaptation in trees and its scale. *Environ. Évid.* **2015**, *4*, 20. [CrossRef]
49. Avagyan, A.B. Correlations between delayed fluorescence of chlorophyll, metabolism and yield of plants. II. Influence of moisture of leaf and temperature condition on delayed fluorescence of leaves. *J. Biophys. Chem.* **2010**, *1*, 52–57. [CrossRef]
50. Sork, V.L.; Sork, K.A.; Hochwender, C. Evidence for local adaptation in closely adjacent sub-populations of northern red oak (*Quercus rubra* L.) expressed as resistance to leaf herbivores. *Am. Nat.* **1993**, *142*, 928–936. [CrossRef] [PubMed]
51. Callow, D.; May, P.; Johnstone, D.M. Tree Vitality Assessment in Urban Landscapes. *Forests* **2018**, *9*, 279. [CrossRef]
52. Mausolf, K.; Härdtle, W.; Jansen, K.; Delory, B.M.; Hertel, D.; Leuschner, C.; Temperton, V.M.; von Oheimb, G.; Fichtner, A. Legacy effects of land-use modulate tree growth responses to climate extremes. *Oecologia* **2018**, *187*, 825–837. [CrossRef] [PubMed]
53. Marqués, L.; Peltier, D.M.P.; Camarero, J.J.; Zavala, M.A.; Madrigal-González, J.; Sangüesa-Barreda, G.; Ogle, K. Disentangling the Legacies of Climate and Management on Tree Growth. *Ecosystems* **2021**, *25*, 215–235. [CrossRef]
54. Boyce, R.L.; Larson, J.R.; Sanford, J.R.L. Phosphorus and nitrogen limitations to photosynthesis in Rocky Mountain bristlecone pine (*Pinus aristata*) in Colorado. *Tree Physiol.* **2006**, *26*, 1477–1486. [CrossRef] [PubMed]
55. Alía, R.; Moro, J.R.; Denis, J.B. Performance of *Pinus pinaster* provenances in Spain: Interpretation of the genotype by environment interaction. *Can. J. For. Res.* **1997**, *27*, 1548–1559. [CrossRef]
56. Cárdenas, A.M.; Gallardo, P. Relationship between insect damage and chlorophyll content in Mediterranean oak species. *Appl. Ecol. Environ. Res.* **2016**, *14*, 477–491. [CrossRef]
57. Matsubara, S.; Chow, W.S. Populations of photoinactivated photosystem II reaction centers characterized by chlorophyll *a* fluorescence lifetime in vivo. *Proc. Natl. Acad. Sci. USA* **2004**, *101*, 18234–18239. [CrossRef]
58. Krause, G.H. Photoinhibition of Photosynthesis. An Evaluation of Damaging and Protective Mechanisms. In *Physiologia Plantarum*; John Wiley & Sons, Ltd.: Hoboken, NJ, USA, 1988; Volume 74, pp. 566–574. [CrossRef]
59. Strasserf, R.J.; Srivastava, A. Govindjee polyphasic chlorophyll *a* fluorescence transient in plants and cyanobacteria. *Photochem. Photobiol.* **1995**, *61*, 32–42. [CrossRef]
60. Pleban, J.R.; Guadagno, C.R.; Mackay, D.S.; Weinig, C.; Ewers, B.E. Rapid Chlorophyll *a* Fluorescence Light Response Curves Mechanistically Inform Photosynthesis Modeling. *Plant Physiol.* **2020**, *183*, 602–619. [CrossRef] [PubMed]
61. Xu, Q.; Ma, X.; Lv, T.; Bai, M.; Wang, Z.; Niu, J. Effects of Water Stress on Fluorescence Parameters and Photosynthetic Characteristics of Drip Irrigation in Rice. *Water* **2020**, *12*, 289. [CrossRef]
62. Zhori, A.; Meco, M.; Brandl, H.; Bachofen, R. In situ chlorophyll fluorescence kinetics as a tool to quantify effects on photosynthesis in *Euphorbia cyparissias* by a parasitic infection of the rust fungus *Uromyces pisi*. *BMC Res. Notes* **2015**, *8*, 698. [CrossRef] [PubMed]

63. Kjelgren, R.; Montague, T. Urban tree transpiration over turf and asphalt surfaces. *Atmos. Environ.* **1998**, *32*, 35–41. [CrossRef]
64. Percival, G.; Schaffert, E.; Hailey, L. Trees in the Rural Landscape. In *Horticulture: Plants for People and Places*; Dixon, G., Aldous, D.E., Eds.; Springer: Berlin/Heidelberg, Germany, 2014; Volume 2.

Disclaimer/Publisher's Note: The statements, opinions and data contained in all publications are solely those of the individual author(s) and contributor(s) and not of MDPI and/or the editor(s). MDPI and/or the editor(s) disclaim responsibility for any injury to people or property resulting from any ideas, methods, instructions or products referred to in the content.